Are the Properties of Shells Ligand Dependent? An ab Initio Study of Mixed $H_3^+Ar_n(H_2)_m$ ($n + m = 6$) Cations

Malgorzata Kaczorowska,[†] Szczepan Roszak,[†,‡] and Jerzy Leszczynski*[,†]

The Computational Center for Molecular Structure and Interactions, Department of Chemistry, Jackson State University, P.O. Box 17910, 1400 J. R. Lynch Street, Jackson, Mississippi 39217, and Institute of Physical and Theoretical Chemistry, Wroclaw University of Technology, Wyb. Wyspianskiego 27, 50-370 Wroclaw, Poland

Received: April 18, 2001; In Final Form: June 19, 2001

The structures and consecutive energies and enthalpies of dissociation reactions were studied theoretically for cations of the general formula $H_3^+Ar_n(H_2)_m$ ($n = 0, 6$; $m = 0, 6$; and, $n + m = 6$). It was found that the extent of modification of the core cation by particular ligands is the main reason for differences between properties of pure and mixed complexes. Since this modification is caused by the core−ligand interactions, the differences in the nature of interactions for binding of argon or molecular hydrogen to the H_3^+ cation are addressed. The vibrational frequencies for the H_3^+ modes were studied as a source of information concerning the environment of the core ion.

I. Introduction

The solvation of ions is one of the basic processes in chemistry. Because of the complexity of interactions and its dynamical nature, this process is far from being understood. A reasonable first-order approximation for the modeling of liquids is the assumption that the solution can be represented as a superposition of interactions within small aggregates, which are the building blocks of the liquid. However, the description of potential surfaces corresponding to clusters is nontrivial, because of the importance of many body interactions. The natural approach to describe the properties of the solution would be to observe the evolution of these properties in ionic clusters, starting from the bare ion and proceeding toward the ion in the bulk solution. The gas phase experiments involving ionic clusters supply data covering species of different degree of complexity.[1] The modern experimental techniques allow for the measurement of properties for the consecutive growth of clusters within the wide range of cluster sizes.[2] Vast data for clusters is available including thermodynamic data, electron affinity properties, and spectroscopic data.[3]

An important group of moieties are clusters where ligands coordinated by an ion are characterized by their negligible intermolecular interactions. In such a case the structure and properties are mostly determined by the central ion.[3] The symmetry of the core ion determines shells that host coordinated ligands (shellvents). The clusters based on the same core and different shellvent molecules often possess similar structures and symmetries. The core ion, however, is modified due to its interactions with the closest neighbors, and such changes affect the further attachment of molecules. The question arises, what would be the effect of replacing one kind of ligand with another? What would be the effect of such a modification on the overall complex structure and properties? The clusters with mixed shellvents have been observed experimentally.[4,5]

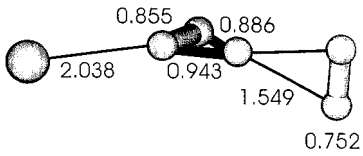

Figure 1. $H_3^+Ar(H_2)$ (C_s) cluster. Distances in angstrom.

In the present study the clusters formed by the H_3^+ cation with coordinated mixed ligands (H_2 molecules and Ar atoms) are investigated. Their structures, thermodynamic properties, and the nature of interactions are presented in this work. The pure complexes $H_2^+Ar_n$ and $H_3^+(H_2)_n$ have already been studied, both experimentally[6,7] and theoretically,[8−12] and may serve as a reference for the present work. The similarity and differences between pure and mixed clusters are emphasized in our study.

II. Theoretical Approach and Computational Details

The calculations presented here were performed by applying the second-order Møller−Plesset perturbation theory (MP2)[13] and the G2 theory[14] in its G2(MP2) version.[15] MP2 calculations were performed utilizing the standard 6-311+G(d,p) basis set.[16−18] No symmetry constraints were imposed during the optimization process, and the geometry searches were performed for a number of possible isomers to ensure the determination of the global minimum. To ensure the proper convergence on flat potential surfaces, the Gaussian "tight" option has been applied. Harmonic vibrational frequencies were calculated for each structure, and only minimum energy species characterized by only real frequencies are reported in this paper. In addition, for each of the considered complexes, a number of transition state structures has been obtained and characterized. The energetically lowest complexes are presented in Figures 1−5. The vibrational frequencies and thermodynamic properties of the studied complexes were calculated by applying the ideal gas, rigid rotor, and harmonic oscillator approximations.[19]

[†] Jackson State University.
[‡] Wroclaw University of Technology.

10.1021/jp011475v CCC: $20.00
Published on Web 07/27/2001

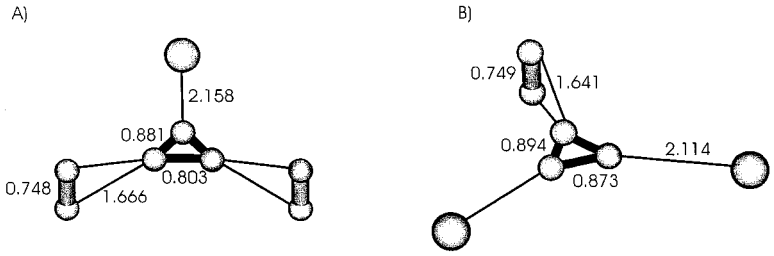

Figure 2. $H_3^+Ar(H_2)_2$ (C_{2v}) and $H_3^+Ar_2(H_2)$ (C_{2v}) clusters. Distances in angstroms.

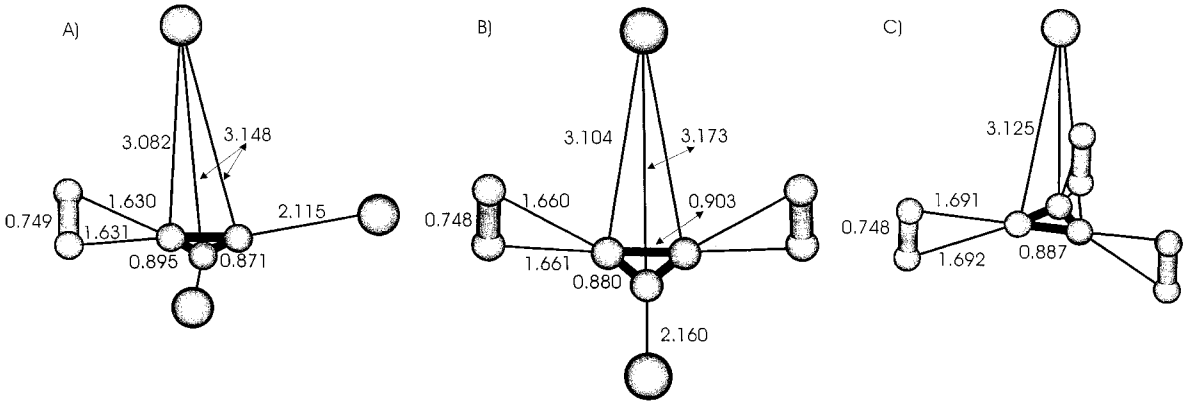

Figure 3. Mixed clusters possess four ligands in shells: (A) $H_3^+Ar_3(H_2)$ (C_{2v}), (B) $H_3^+Ar_2(H_2)_2$ (C_{2v}), and (C) $H_3^+Ar(H_2)_3$ (C_{3v}). Distances in angstroms.

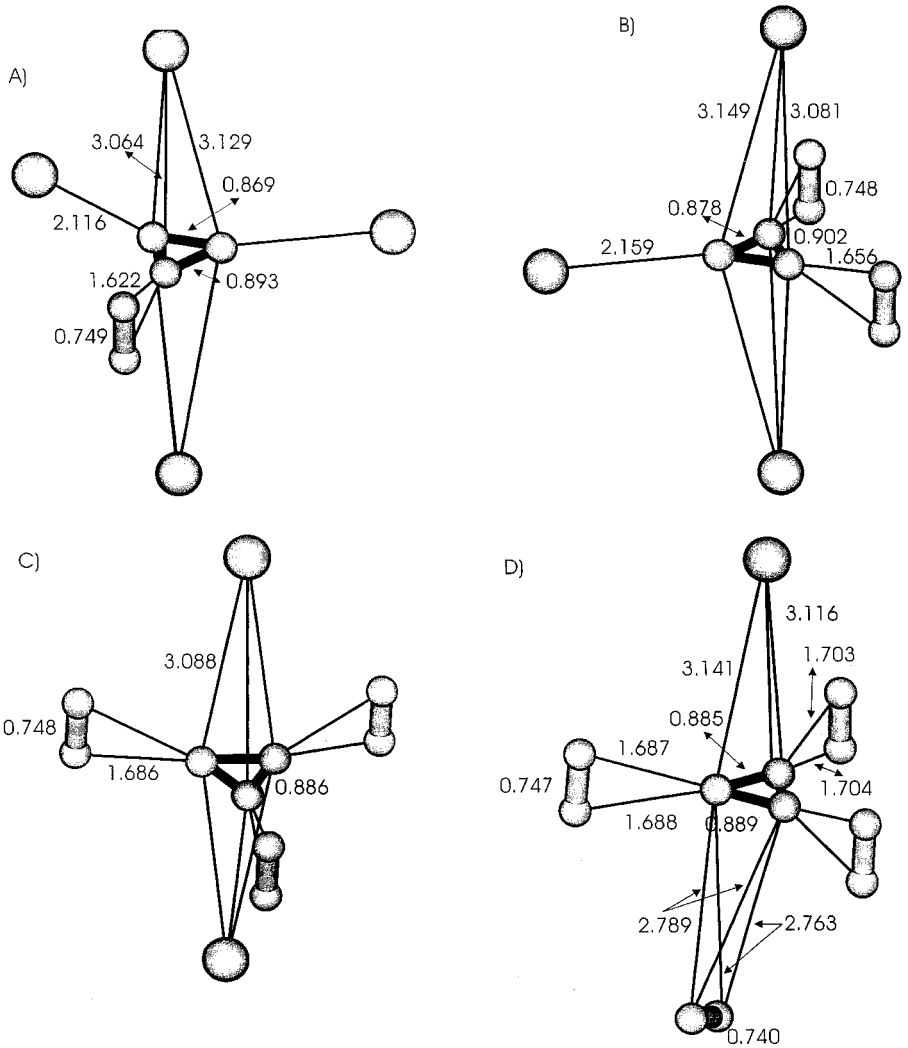

Figure 4. Mixed clusters possess five ligands in shells: (A) $H_3^+Ar_4(H_2)$ (C_{2v}), (B) $H_3^+Ar_3(H_2)_2$ (C_{2v}), (C) $H_3^+Ar_2(H_2)_3$ (D_{3h}), and (D) $H_3^+Ar(H_2)_4$ (C_s). Distances in angstrom.

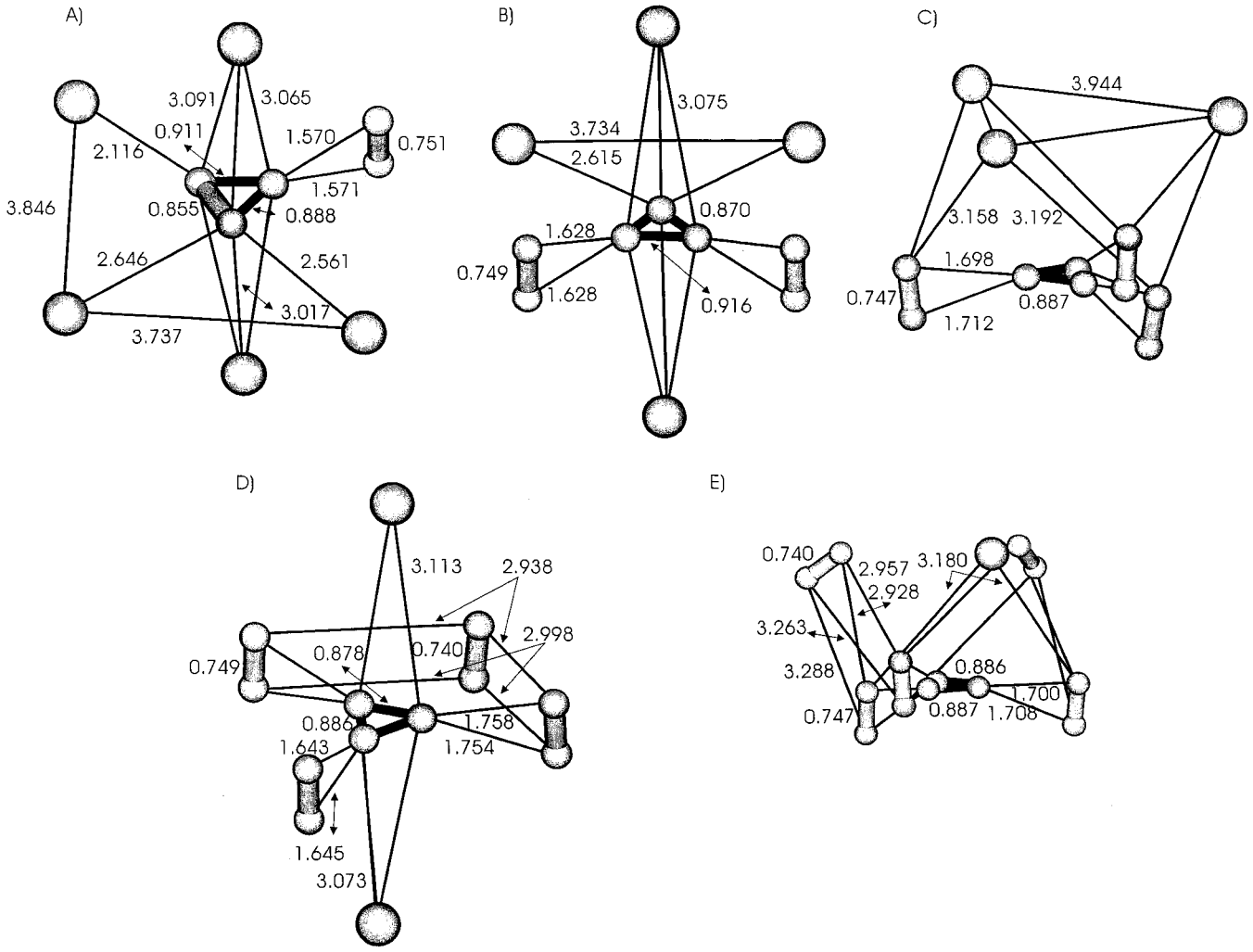

Figure 5. Mixed clusters including six ligands in shells: (A) $H_3^+Ar_5(H_2)$ (C_s), (B) $H_3^+Ar_4(H_2)_2$ (C_{2v}), (C) $H_3^+Ar_3(H_2)_3$ (C_3), (D) $H_3^+Ar_2(H_2)_4$ (C_s), and (E) $H_3^+Ar(H_2)_5$ (C_1). Distances in angstrom.

The total interaction energy

$$\Delta E_{TOT} = E_{AB} - E_A - E_B$$

has been decomposed

$$\Delta E_{TOT} = \Delta E_{SCF} + \epsilon_{disp}^{(20)}$$

into Hartree−Fock and dispersion parts. The applied SCF energy decomposition was performed within the variational−perturbational scheme corrected for the basis set superposition error.[20] In the above scheme ΔE_{HF} was partitioned into the electrostatic ($\epsilon_{el}^{(10)}$) and Heitler−London exchange (ϵ_{ex}^{HL}) first-order components and the higher order delocalization (ΔE_{del}^{HF}) term. The delocalization energy accounts for the charge transfer, induction, and other higher order Hartree−Fock terms.[21,22] The main contribution to the correlation energy is due to the second-order Hartree−Fock dispersion energy ($\epsilon_{disp}^{(20)}$).

The calculations of energies and thermodynamic properties were carried out using the Gaussian 98 code.[23] The interaction energy decomposition was performed by applying the modified version[24] of the Gamess (version December 98) code.[25] The MP2 approach has been previously applied for the study of O^-Ar_n and $H_3^+Ar_n$ systems, and the results were tested against the advanced MP4 and coupled cluster (CCSD(T)) approaches and yield very encouraging results.[9,26]

III. Structures and Energetics of $H_3^+Ar_n(H_2)_m$ Clusters

The first occupied shell (A), characterized for the both pure $H_3^+(H_2)_n$ and $H_3^+Ar_n$ clusters, is located on the H_3^+ plane, with H_2 or Ar ligands attached to the triangle vertexes. In both cases the fully occupied shells possess D_{3h} symmetry. The mixed complexes form similar structures (Figures 1 and 2) with the symmetry plane defined by the H_3^+ ring. The $H_3^+Ar_2(H_2)$ and $H_3^+Ar(H_2)_2$ mixed complexes (Figure 2) are of C_{2v} symmetry, as derived from the D_{3h} core symmetry destroyed by the perturbation imposed by the replacement of an ligand. Significant energy differences exist between isomers with the first or second shell occupied (Figure 7), and although isomers with three ligands coordinated to both not fully occupied shells A and B are possible, they are unlikely to be observed.

The energetical factor becomes important when the process of filling the second shell is initialized (Figure 3). Assuming the additivity of experimental consecutive enthalpies of formation measured for pure clusters[6,7] (the additive rule), the occupation A(H_2,Ar,Ar)B(Ar) leads to the lowest total enthalpy. Although the above assumption may serve only as a rough estimation of the isomer stability, the most favorable structure of $H_3^+Ar_3(H_2)$ determined theoretically agrees with the assumed pattern of occupation. The attachment of the first H_2 to H_3^+ is the most profitable, and at least one position in the A shell is occupied by the hydrogen molecule in all mixed structures determined in this work.

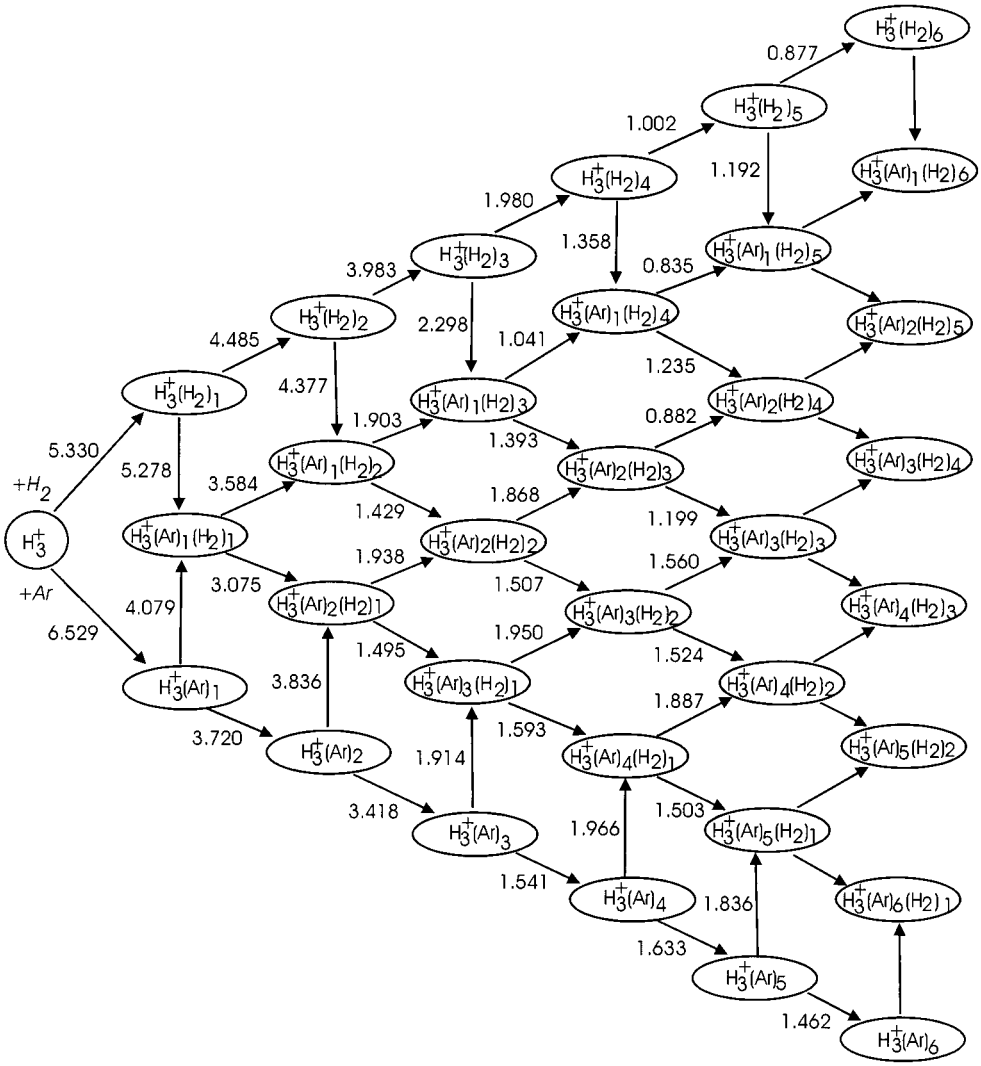

Figure 6. Consecutive energies of the formation (D_e) of $H_3^+Ar_n(H_2)_m$ ($n = 0, 6$; $m = 0, 6$; and $n + m = 6$) clusters. Energies in kcal/mol.

The complex with the $2Ar+2H_2$ stoichiometry (Figure 3b) follows the occupation pattern of $A(H_2,Ar,H_2)B(Ar)$. This structure is energetically slightly less favorable than the $A(H_2,Ar,Ar)B(H_2)$ sequence predicted from experimental data for pure clusters as the most preferable. The small energy difference estimated for the above sequences lies within the error bars of the experimental data. More likely, however, the energy differences result from different natures of interaction in pure and mixed clusters. The small energy difference (less than 0.5 kcal/mol as estimated by the above procedure) indicates that both isomers may exist simultaneously. In the case of the $H_3^+Ar(H_2)_3$ moiety, two possible isomers also lie within 0.5 kcal/mol on the potential energy surface. The lowest energy isomer possesses the $A(H_2,H_2,H_2)B(Ar)$ occupation (Figure 3c) and has the perfect C_{3v} symmetry. In all studied complexes, the second shell always possesses the Ar atom located above H_3^+ (the shell B).

The general feature of clusters with five shellvated ligands is the preferable occupation of the B shell by Ar and occupation of the A shell by H_2 (Figure 4). The additivity rule again indicates the possibility of the existence of energetically close isomers (two in the case of $H_3^+Ar_4(H_2)$ and $H_3^+Ar(H_2)_4$ and three for $H_3^+Ar_2(H_2)_3$ and $H_3^+Ar_3(H_2)_2$ moieties).

The complexes containing six members in shells are especially interesting since pure $H_3^+Ar_6$ and $H_3^+(H_2)_6$ clusters possess different structures. In $H_3^+Ar_6$ the A shell hosts four Ar atoms while the $H_3^+(H_2)_6$ cluster adopts the A(3)B(3) occupation. The energetically lowest isomers of the mixed complexes follow one of these sequences (Figure 5). $H_3^+Ar_5(H_2)$, $H_3^+Ar_4(H_2)_2$, and $H_3^+Ar_2(H_2)_4$ clusters form the A(4) shell with the B shell being always occupied by Ar atoms. However, the $H_3^+Ar_3(H_2)_3$ and $H_3^+Ar(H_2)_5$ complexes follow the A(3)-B(3) occupation pattern with the A shell filled totally by hydrogen molecules. In the all determined complexes, whenever it is possible, the hydrogen molecules occupy the A shell.

The interactions with ligands govern the ability of the H_3^+ core to bond the consecutive ligands. When argon atoms are present in mixed clusters, the binding in general is enhanced for consecutive H_2 as well as Ar ligands (Figure 6). H_2 lowers the reactivity of the complex. The large difference between H_2 and Ar masses highly influences the enthalpies of their attachment. The enthalpy correction to the dissociation energy is positive in the case of the H_2 attachment and negative for the Ar attachment.

IV. Nature of Bonding

The differences in the nature of interactions observed in the mixed clusters originate from the differences between argon atoms and H_2 molecules for their affinity to the H_3^+ ring. The affinity is closely related to the charge on the H_3^+ core. The shellvated ligands interact with each other through alternation

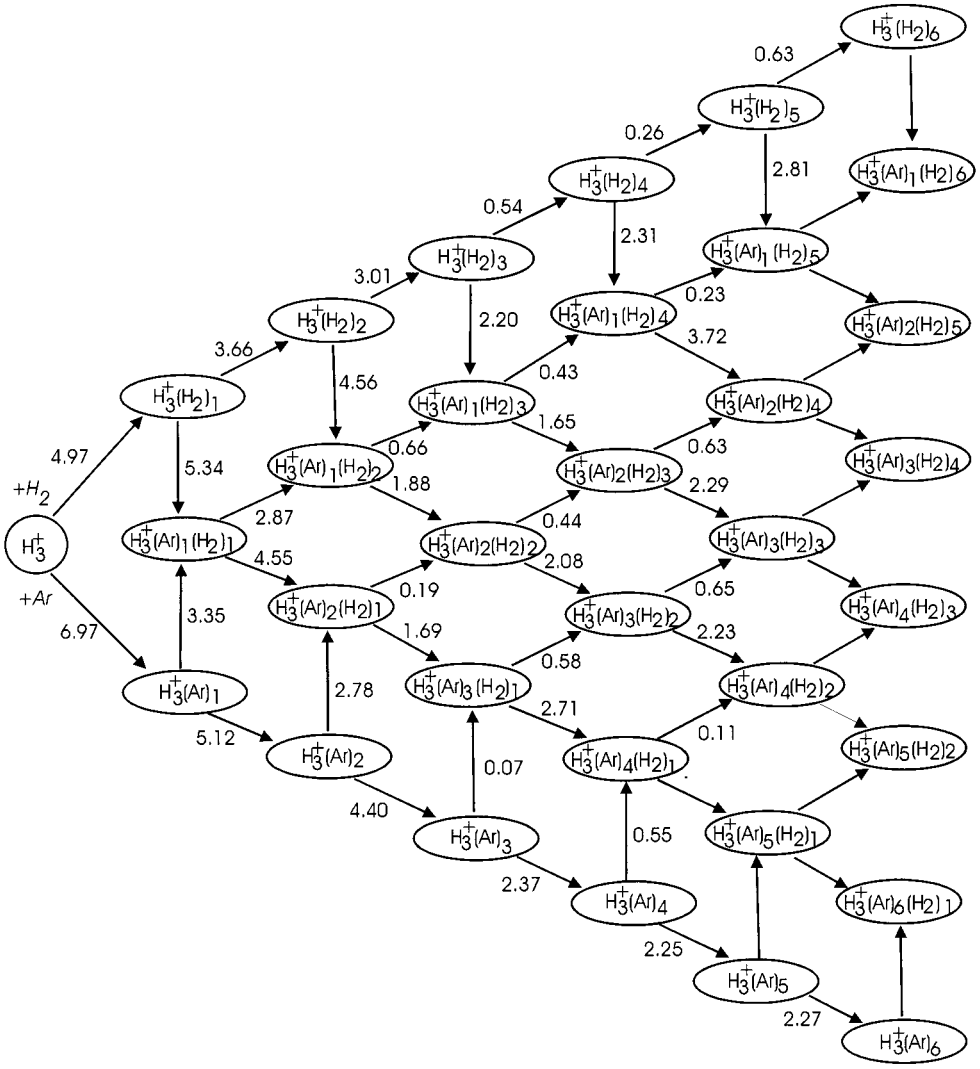

Figure 7. Consecutive enthalpies of the dissociation reactions ($\Delta H_{n+m,n+m-1}$) for $H_3^+Ar_n(H_2)_m$ ($n = 0, 6$; $m = 0, 6$; and $n + m = 6$) clusters. Energies in kcal/mol.

of the H_3^+ properties. Because of the lower ionization potential ($IP_{H2} = 15.42$, $IP_{Ar} = 15.79$ eV),[27] H_2 donates more electronic density to H_3^+ (Figure 8), thereby lowering its charge and binding power toward consecutive ligands. Although the consecutive binding of hydrogen molecules reduces the charge transferred from H_2 to the H_3^+ ring, this transfer is always higher compared to the transfer from similar shell formed by Ar atoms. The above conclusion are also supported by the values of calculated electrostatic interaction energies ($\epsilon_{el}^{(10)}$) (Table 1). The replacement of H_2 molecules by Ar atoms enhances the energy of interactions of consecutive ligands due to the smaller density transfer to H_3^+. In the case of interacting Ar atoms, the dispersion energy ($\epsilon_{disp}^{(20)}$) is always higher than the total SCF interaction energy. This is true regardless of the origin of the Ar location (A or B shell). The interactions of H_2 with the core are characterized by much larger SCF components (with the main contribution being an electrostatic term) rather than being the consequence of the correlation energy. The H_2 molecule has a higher impact on the bonding of neighbors. In the case of two ligands present in the A shell, the energy of H_2 dissociation from $H_3^+Ar(H_2)$ is higher compared to the dissociation energy of the second H_2 from $H_3^+(H_2)_2$. On the other hand, H_2 as the more aggressive reagent weakens the neighboring H_3^+-Ar bond. This effect is quite visible in comparison with the H_3^+-$Ar(H_2)$ and $H_3^+Ar_2$ isomers (Table 2). Similar effects are also

TABLE 1: Interaction Energy Decomposition[a]

complex	interacting fragment	$\epsilon_{el}^{(10)}$	ϵ_{ex}^{HL}	ΔE_{del}	ΔE_{SCF}	$\epsilon_{disp}^{(20)}$	ΔE_{TOT}
$H_3^+(H_2)_2$	H_2	−4.21	12.77	−11.39	−2.83	−1.86	−4.69
$H_3^+Ar(H_2)$	H_2	−4.36	13.47	−13.45	−4.34	−2.11	−6.45
	Ar	−0.81	9.04	−9.33	−1.11	−0.71	−1.82
$H_3^+Ar_2$	Ar	−0.87	10.80	−11.27	−1.34	−1.83	−3.17
$H_3^+(H_2)_3$	H_2	−3.39	8.99	−7.83	−2.23	−1.50	−3.73
$H_3^+Ar(H_2)_2$	H_2	−3.54	9.54	−8.82	−2.81	−1.72	−4.57
	Ar	−0.66	6.19	−6.30	−0.77	−0.54	−1.31
$H_3^+Ar_2(H_2)$	H_2	−3.71	10.29	−9.64	−3.06	−2.00	−5.06
	Ar	−0.72	7.13	−7.22	−0.82	−1.41	−2.23
$H_3^+Ar_3$	Ar	−0.78	8.06	−8.12	−0.85	−1.72	−2.57
$H_3^+Ar(H_2)_3$	H_2	−3.41	8.92	−7.92	−2.41	−1.74	−4.15
	Ar	−0.20	0.98	−1.18	−0.40	−0.59	−0.99
$H_3^+Ar_2(H_2)_2$	H_2	−3.65	9.85	−8.87	−2.67	−1.85	−4.52
	Ar(B)[b]	−0.21	1.04	−1.17	−0.34	−0.53	−0.87
	Ar(A)	−0.69	6.22	−6.19	−0.66	−1.34	−2.00
$H_3^+Ar_3(H_2)$	H_2	−3.89	10.83	−9.88	−2.93	−1.37	−4.30
	Ar(B)	−0.21	1.08	−1.13	−0.26	−0.57	−0.83
	Ar(A)	−0.76	7.19	−7.12	−0.69	−1.60	−2.29
$H_3^+Ar_4$	Ar(B)	−0.22	1.09	−1.04	−0.16	−0.51	−0.68
	Ar(A)	−0.83	8.22	−8.08	−0.70	−1.78	−2.48

[a] The HF interaction energy has been decomposed into electrostatic ($\epsilon_{El}(10)$), exchange ($\epsilon_{Ex}HL$), and delocalization (ΔE_{del}) terms. ΔE_{SCF} is the total Hartree−Fock interaction; $\epsilon_{Disp}(20)$ denotes the dispersion energy. Energies are in kcal/mol [b] The shell of interacting molecule or atom.

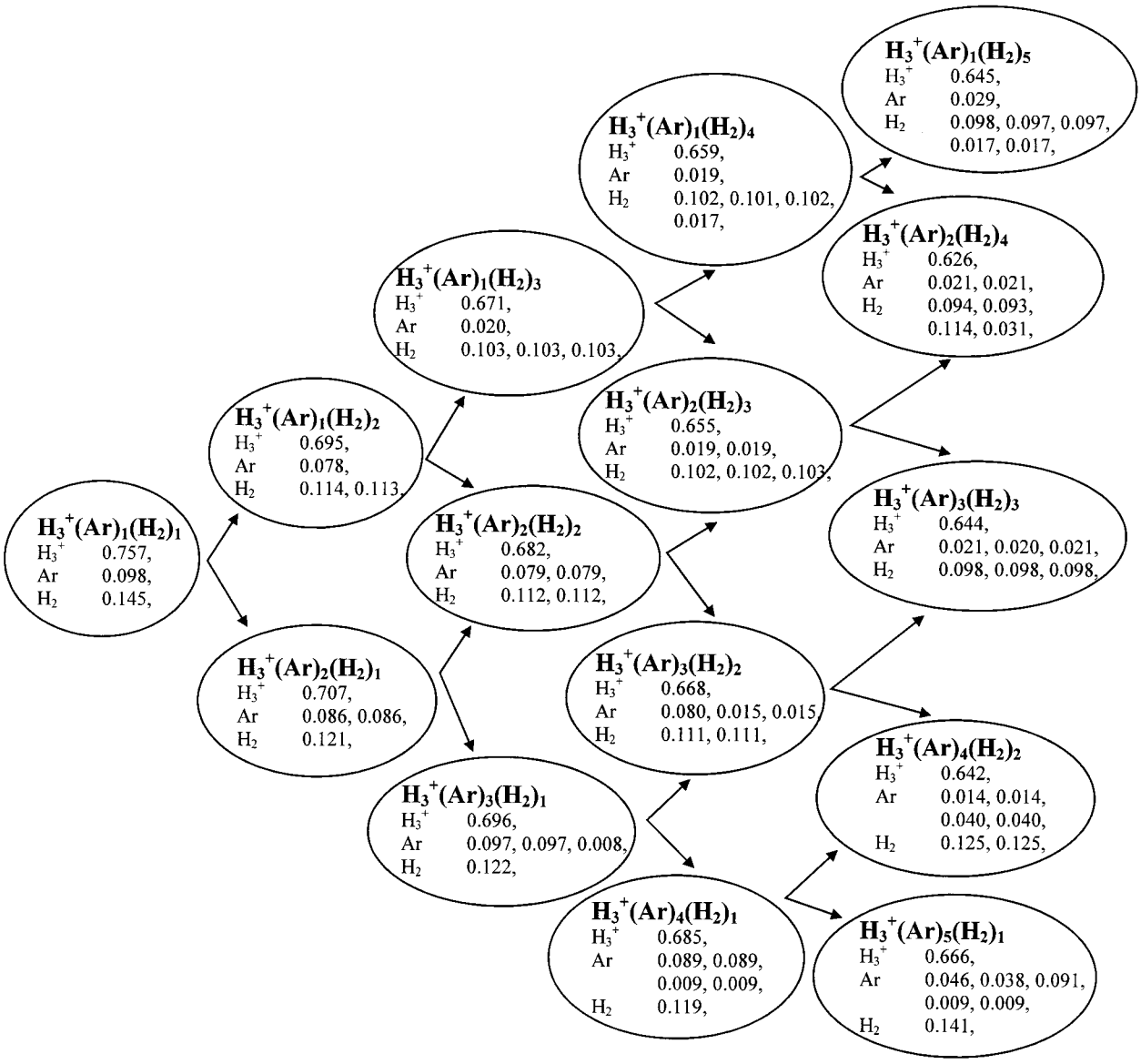

Figure 8. Atomic charges for the mixed $H_3^+Ar_n(H_2)_m$ ($n = 1, 5$; $m = 1, 5$) clusters calculated within the Mulliken population analysis. Atomic and molecular charges in electrons.

observed in the larger mixed clusters. The presence of H_2 molecules always weakens the other H_3^+-Ar bonds.

An analysis of the nature of interactions, based on the intermolecular interactions concept, assumes the same geometry for the parent complex and its subunits. However, the addition of a ligand (atom or molecule) to the existing structure often leads to a dramatic structural rearrangement when the product is formed. In the reaction $H_3^+Ar_2(H_2) + H_2 = H_3^+Ar_2(H_2)_2$ (Figures 2b and 3b), the Ar atom moves from the A shell to the B shell, allowing the reacting H_2 to form the energetically preferred structure. The energy of such structural deformation (ΔE_{def}) is often comparable to interaction energies and should be account for.

V. Vibrational Properties of the H_3^+ Core

The experiments performed by Boo and Lee for the $CH_3^+(H_2)_n$ cations[28] indicate that the C−H stretching vibrations of the CH_3^+ core were the source of information concerning the structure of the H_2 environment. It was shown that the same applies to the $H_3^+Ar_n$ complexes.[9]

The calculated harmonic vibrational frequencies reveal details of structure and bonding in the studied species. The first effect observed in the mixed complexes is the splitting of the deformation bands due to the lowering of symmetry due to the perturbation imposed by different ligands in shells (Table 2). The frequencies corresponding to the H_3^+ fragment in the complex are significantly lower compared to those of the bare H_3^+ cation. As expected, due to the higher interaction energy, the H_2 molecule has a larger impact on the vibrational frequencies than does the Ar atom. The largest modifications of vibrational frequencies compared to pure clusters originate from interactions within the first shell. More complex clusters with their overall weaker bonding show smaller impact on vibrations, and such clusters gradually restore vibrational characteristics of the parent core ion. The effect of the stabilization of the core cation was also observed in the experiments of Boo and Lee with $CH_3^+(H_2)_n$ species.[28]

VI. Conclusions

The molecular structures of mixed clusters of the general formula $H_3^+Ar_n(H_2)_m$ were studied. The determined geometries

TABLE 2: Vibrational Frequencies (in cm^{-1}) for the Deformation and Ring Breathing Modes of the H_3^+ Fragment in Different Size Clusters[a]

cation	symmetry	deformation I	deformation II	ring breathing[b]
H_3^+	D_{3h}	2794 (2520)		3494 (3165)
$H_3^+(H_2)_2$	C_{2v}	2252 (2040)	2554 (2214)	3359 (3043)
$H_3^+Ar(H_2)$	C_{2v}	2264 (2051)	2514 (2278)	3379 (3061)
$H_3^+Ar_2$	C_{2v}	2290 (2075)	2529 (2291)	3360 (3044)
$H_3^+(H_2)_3$	D_{3h}	2491 (2257)		3266 (2959)
$H_3^+Ar(H_2)_2$	C_{2v}	2447 (2217)	2524 (2287)	3287 (2978)
$H_3^+Ar_2(H_2)$	C_{2v}	2457 (2226)	2510 (2274)	3296 (2986)
$H_3^+Ar_3$	D_{3h}	2488 (2254)		3293 (2983)
$H_3^+(H_2)_4$	C_{2v}	2489 (2255)	2510 (2274)	3279 (2971)
$H_3^+Ar(H_2)_3$	C_{3v}	2501 (2266)		3281 (2973)
$H_3^+Ar_2(H_2)_2$	C_{2v}	2453 (2222)	2530 (2292)	3299 (2989)
$H_3^+Ar_3(H_2)$	C_{2v}	2462 (2230)	2516 (2279)	3310 (2999)
$H_3^+Ar_4$	C_{3v}	2500 (2265)		3308 (2997)

[a] The frequencies scaled to reproduce experimental H_3^+ frequencies (scaling factor 0.902) are given in parentheses. [b] Experimental values for H_3^+: deformation 2521.3, ring breathing 3178.2 cm^{-1}, from ref 29.

resemble those found in pure $H_3^+Ar_n$ and $H_3^+(H_2)_n$ complexes, indicating the major role of the core ion in the determination of the structure of shells. The occupation of shells by different ligands lowers the symmetry. Pure clusters $H_3^+Ar_6$ and $H_3^+(H_2)_6$ follow different occupation patterns, e.g., A(4)B(2) and A(3)B(3), respectively. The mixed species follow the former or the latter pattern depending on the composition of the moiety. The energetical differences between isomers are small, thus leading to a number of possible isomers.

The interaction energy partitioning indicates the significant differences between the nature of H_2 and Ar binding to the H_3^+ core. The predominant interactions for H_2 are electrostatic in nature, while Ar atoms are bonded via the dispersion forces. The H_2 molecules and Ar atoms influence the binding of each other through the modification of the charge on the H_3^+ ring as an effect of the electronic density transfer. The shellvation of the H_3^+ cation weakens the bonding within the H_3^+ skeleton. This effect is the largest for the smallest clusters (the first shell clusters). The formation of larger complexes stabilizes the cation.

Acknowledgment. This work was facilitated in part by NSF grant 9805465 and 9706268, Wroclaw University of Technology Grant No. 341-831, and the Army High Performance Computing Research Center under the auspices of the Department of the Army, Army Research Laboratory cooperative agreement number DAAH04-95-2-0003/contract number DAAH04-95-C-0008. This work does not necessarily reflect the policy of the government, and no official endorsement should be inferred. We thank the Mississippi Center for Supercomputing Research, Poznan, and Wroclaw Supercomputing and Networking Centers, and the Interdisciplinary Center for Mathematical and Computational Modeling of the Warsaw University for a generous allotment of computer time.

References and Notes

(1) Hiraoka, K.; Yamabe, S. In *Dynamics of Excited Molecules*; Kuchitsu, K., Ed.; Studies in Physical and Theoretical Chemistry, Vol. 82; Elsvier Science: Amsterdam, 1994.

(2) Coe, J. V.; Lee, G. H.; Eaton, J. G.; Arnold, S. T.; Sarkas, H. W.; Bowen, K. H.; Ludewigt, C.; Haberland, H.; Worshow, D. R. *J. Chem. Phys.* **1990**, *92*, 3980.

(3) Roszak, S.; Leszczynski, J. In *Computational Chemistry: Reviews of Current Trends*; Leszczynski, J., Ed.; World Scientific: Singapore, 2001; Vol. 6.

(4) Hiraoka, K.; Fujimaki, S.; Nasu, M.; Minamitsu, A.; *J. Chem. Phys.* **1997**, *107*, 2550.

(5) Boo, D. W.; Lee, Y. T. *Int. J. Mass Spectrosc. Ion Processes* **1996**, *159*, 209.

(6) Hiraoka, K. J. *Chem. Phys.* **1987**, *87*, 4048.

(7) Hiraoka, K.; Mori, T. *J. Chem. Phys.* **1989**, *91*, 4821.

(8) Ignacio, E. W.; Yamabe, S. *Chem. Phys. Lett.* **1998**, *287*, 563.

(9) Kaczorowska, M.; Roszak, S.; Leszczynski, J. *J. Chem. Phys*. **2000**, *113*, 563.

(10) Barbatti, M.; Jalbert, G.; Nascirnento, M. A. C. *J. Chem. Phys*. **2001**, *114*, 7066.

(11) Barbatti, M.; Jalbert, G.; Nascirnento, M. A. C. *J. Chem. Phys*. **2000**, *113*, 4230.

(12) Farizon, B.; Farizon, M.; Razafinjanahary, H.; Chermette, H. *Phys. Rev. B* **1999**, *60*, 3821.

(13) Møller, C.; Plesset, M. S. *Phys. Rev.* **1934**, *46*, 618.

(14) Curtiss, L. A.; Raghavachari, K.; Trucks, G. W.; Pople, J. A.*J. Chem. Phys*. **1991**, *94*, 7221.

(15) Curtiss, L. A.; Raghavachari, K.; G. W.; Pople, J. A. *J. Chem. Phys.* **1993**, *98*, 1293.

(16) Krishnan, R.; Binkley, J. S.; Seeger, R.; Pople, J. A. *J. Chem. Phys*. **1980**, *72*, 650.

(17) McLean, A. D.; Chandler, G. S. *J. Chem. Phys*. **1980**, *72*, 5639.

(18) Clark, T.; Chandrasekhar, J.; Schleyer, P. v. R. *J. Comput. Chem.* **1983**, *4*, 294.

(19) Davidson, N. *Statistical Mechanics*; McGraw-Hill: New York, 1962.

(20) Sokalski, W. A.; Roszak, S.; Pecul, K. *Chem. Phys. Lett*. **1988**, *153*, 153.

(21) Jeziorski, B.; van Hemert, M. C. *Mol. Phys.* **1976**, *31*, 713.

(22) Chalasinski, G.; Szczesniak, M. M. *Mol. Phys*. **1988**, *63*, 205.

(23) Frisch, M. J.; Trucks, G. W.; Schlegel, H. B.; Scuseria, M. A.; Robb, M. A.; Zakrzewski, V. G.; Montgomery, J. A.; Stratman, R. E.; Burant, J. C.; Daprich, S.; Millam, J. M.; Daniels, A. D.; Kudin, K. N.; Strain, M. C.; Farkas, O.; Tomasi, J.; Barone, V.; Cossi, M.; Cammi, R.; Mennucci, B.; Pomelli, C.; Adamo, C.; Clifford, S.; Ochterski, J.; Petersson, G. A.; Ayala, P. Y.; Ciu, Q.; Morokuma, K.; Malick, D. K.; Rabuck, A. D.; Raghavachari, K.; Foresman, J. B.; Cioslowski, J.; Oritz, J. V.; Stefanov, B. B.; Liu, G.; Liashenko, A.; Piskorz, P.; Komaromi, I.; Gomperts, R.; Martin, R. L.; Fox, D. J.; Keith, T. A.; Al-Laham, M. A.; Peng, C. Y.; Nanayakkara, Gonzales, C.; A.; Challacombe, M.; Gill, P. M. W.; Johnson, B. G.; Chen, Wong, M. W.; V. G.; Andres, J. L.; Head-Gordon, M.; Replogle, E. S.; Pople, J. A.; *Gaussian98*, revision A.7; Gaussian, Inc.: Pittsburgh, PA, 1995.

(24) Gora, R. W.; Roszak, S.; Leszczynski, J. *JSU Preprint*, 2000.

(25) Schmidt, M. S.; Baldridge, K. K.; Boatz, J. A.; Elbert, S. T.; Gordon, M. S.; Jensen, J. H.; Koseki, S.; Matsunaga, N.; Nguyen, K. A.; Su, S. J.; Windus, T. L.; Dupuis, M.; Montgomery, J. A. *J. Comput. Chem.* **1993**, *14*, 1347.

(26) Roszak, S.; Gora, R. W.; Leszczynski, J. *Chem. Phys. Lett*. **1999**, *313*, 198.

(27) *Handbook of Chemistry and Physics*, Lide, D. R., Ed.; CRC Press: Boca Raton, FL, 1998).

(28) Boo, D. W.; Lee, Y. T. *J. Chem. Phys*. **1998**, *103*, 520.

(29) Jackoy, M. E. *J. Phys. Chem. Ref. Data* Monogr. 3.